Journal of Aerosol Science 134 (2019) 72–79

Contents lists available at ScienceDirect

Journal of Aerosol Science

journal homepage: www.elsevier.com/locate/jaerosci

Design and evaluation of a high-flowrate nanoparticle respiratory deposition (NRD) sampler

Theresa I. Szabo McCollom[a], Larissa V. Stebounova[a], Jae Hong Park[b], Vicki H. Grassian[c], Natalia I. Gonzalez-Pech[c], Thomas M. Peters[a,*]

[a] Department of Occupational and Environmental Health, The University of Iowa, Iowa City, IA, USA
[b] School of Health Sciences, Purdue University, West Lafayette, IN, USA
[c] Department of Chemistry and Biochemistry, University of California San Diego, La Jolla, CA, USA

ARTICLE INFO

Keywords:
Nanoparticle
Respiratory
Deposition
Sampler
Diffusion
Exposure*Keywords:*
Nanoparticle high-flow sampler
Respiratory deposition curve
Impactor
Diffusion stage
Collection efficiency
Pressure drop

ABSTRACT

A high-flow (10 L/min) nanoparticle respiratory deposition (NRD) sampler was designed and evaluated to achieve reduced limits of quantification (LOQs) for metal nanoparticles. The high-flow NRD consists of an inlet, impactor stage, diffusion stage, and a final filter. An impactor stage with 12 nozzles was designed from theory to achieve a cut-off diameter of 300 nm at 50% particle collection efficiency (d_{50}). Various depths of 37-mm-diameter polyurethane foam cylinders were tested for the diffusion stage to obtain a collection efficiency curve similar to the deposition of nanoparticles in the human respiratory tract, known as the nanoparticulate matter (NPM) criterion. The objective for the final filter was a collection efficiency of near 100% with minimal pressure drop. The collection efficiencies by size and pressure drops were measured for all NRD sampler components. The final design of the impactor stage nozzle achieved a d_{50} of 305 nm. The collection efficiency for the diffusion stage with a depth of 7 cm when adjusted for presence of the impactor was the closest to the NPM curve with a R^2 value of 0.96 and d_{50} of 43 nm. Chemical analysis of the metal content for foam affirmed that the high-flow NRD sampler required less sampling time to meet metal LOQs than the 2.5 L/min NRD sampler. The final filter with a modified support pad had a collection efficiency near 100%. The overall pressure drop of the sampler of 8.5 kPa (34 in. H_2O) could not be handled by commercial personal sampling pumps. Hence the high-flow NRD sampler can be used as an area sampler or without the final filter for collection of nanoparticles.

1. Introduction

Nanoparticles, or particles with at least one dimension smaller than 100 nm, are increasingly used in consumer products. Workers are at risk of exposure to nanoparticles during their production and when incorporating them into products. Traditionally, industrial hygienists use size-selective personal samplers to assess workplace exposures to aerosols. These samplers are designed to collect only those particles that penetrate into a certain region of the respiratory system. The American Conference of Governmental Industrial Hygienists (ACGIH) specifies collection criteria for inhalable, thoracic and respirable samplers (ACGIH, 2019). Respirable samplers collect the smallest size fraction with a cut-off diameter (d_{50}) of 4 μm. Nanoparticles are collected in these samplers, but their mass is often obscured by the mass of larger particles.

The National Institute of Occupational Safety and Health (NIOSH) recommends exposure monitoring with two respirable samplers

* Corresponding author. 145 N Riverside Drive, S325 CPHB, Department of Occupational and Environmental Health, University of Iowa, Iowa City, IA, 52242, USA.
E-mail address: thomas-m-peters@uiowa.edu (T.M. Peters).

https://doi.org/10.1016/j.jaerosci.2019.04.019
Received 7 March 2019; Received in revised form 29 April 2019; Accepted 29 April 2019
Available online 30 April 2019
0021-8502/

simultaneously for carbon nanotubes/nanofibers (NIOSH, 2013) and nano-sized titanium dioxide (NIOSH, 2011). One of the respirable samples is analyzed by bulk chemical analysis, whereas the other is analyzed by microscopy to determine the portion in the nano-size fraction. Size-selective personal samplers have been developed to collect nanoparticles apart from larger particles, thereby eliminating the need for microscopy and a duplicate respirable sample. Tsai et al. (2012) described the Personal Nanoparticle Sampler (PENS), which consists of a respirable cyclone and a micro-orifice impactor with a d_{50} of 100 nm (Zhou et al., 2014). This sampler uses a rotating impaction stage to avoid particle bounce and has been used to sample nanoparticles apart from larger particles in the workplace (Thompson, Chen, Wang, & Pui, 2015). Thongyen et al. (Thongyen, Hata et al., 2015) developed a $PM_{0.1}$ personal sampler that allows only 100 nm and smaller particles to pass through a layer of mesh to a final filter.

The Nanoparticle Respiratory Deposition (NRD) sampler collects nanoparticles separately from larger respirable particles, operating at an airflow rate of 2.5 L/min (Cena et al., 2011). The commercially-available version of the NRD sampler (ZA0075, Zefon International, Inc., Ocala, FL) uses a respirable cyclone, followed by an impactor stage that removes particles larger than 300 nm, and a diffusion stage consisting of eight nylon mesh layers. With this arrangement, nanoparticles smaller than 300 nm are collected on the diffusion screens in a way that mimics their deposition within the respiratory tract (Cena et al., 2011). In a newer version of the 2.5 L/min NRD sampler, polyurethane foam replaces nylon meshes to achieve lower limits of quantification, particularly for titanium (Mines et al., 2016). The relatively low sampling airflow rates of these samplers necessitate long sampling times to collect sufficient mass of nanoparticles for quantification.

The objective of this study was to design a high-flow (10 L/min) NRD sampler that collects nanoparticles following NPM criterion resembling particle deposition in human lungs. To meet the objective, we designed the high-flow (10 L/min) NRD sampler with the same target collection efficiencies as the low-flow (2.5 L/min) NRD sampler. The collection efficiency for each of the design elements was evaluated and pressure demands were measured to ensure the samplers' compatibility with a personal pump.

2. Materials and methods

2.1. NRD sampler

The high-flow NRD sampler consists of four principal design elements as shown in Fig. 1a: inlet; impactor stage; diffusion stage; and final filter. The dimensions of the high-flow NRD are 150 mm in length by 42 mm in width, and its weight is 165 g. The inlet and

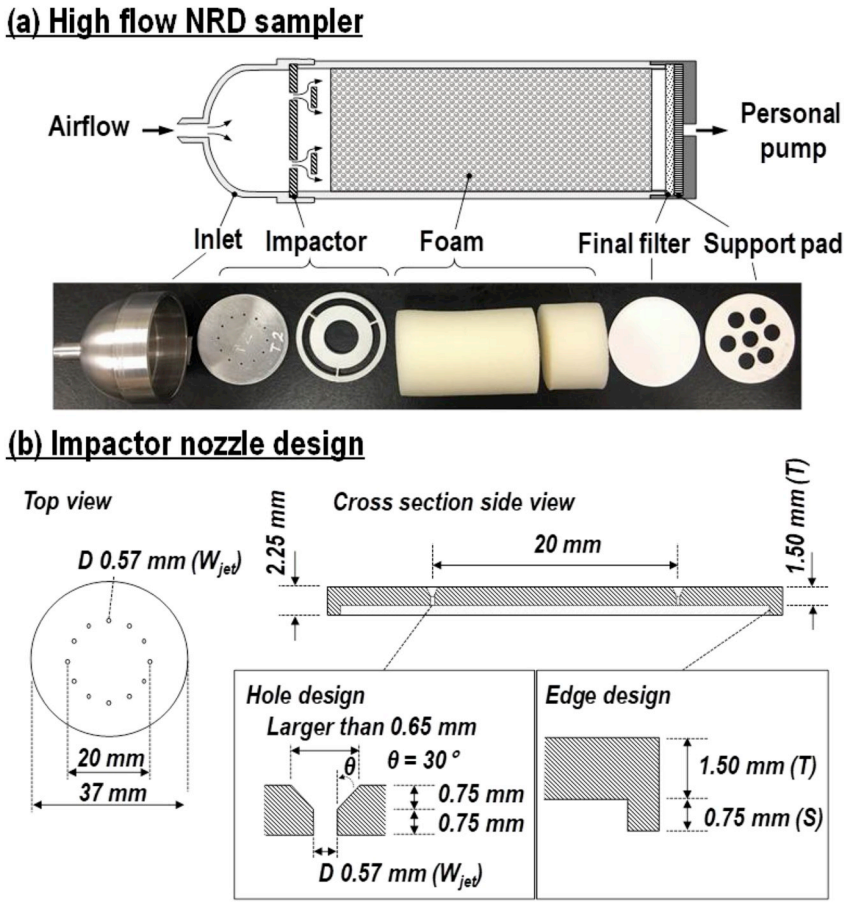

Fig. 1. High-flow NRD sampler design (a), and schematic diagram of impactor nozzle section (b).

Table 1
Design specifications of the impactor nozzle sections. Each section had 12 round nozzles.

	Nozzle 1	Nozzle 2	Nozzle 3
W_{nozzle} (± SD), mm	0.566 (± 0.144)	0.573 (± 0.120)	0.626 (± 0.008)
T/W_{nozzle}	2.23	2.53	1.87
S/W_{nozzle}	1.73	1.40	1.68
Re	2057	2021	1117
V, cm/s	5497	5286	2641
Measured d_{50}, nm	305	328	406

housing for the impaction and diffusion stages were machined from an aluminum alloy. The holder for the final filter is a standard 37-mm filter cassette holder. When air is drawn through the sampler, particles larger than 300 nm are removed due to impaction on a greased collection plate. The remaining airborne particles are passed into a polyurethane foam, which collects particles via diffusion with collection efficiency following the nano-particulate matter (NPM) criterion (Cena et al., 2011). This criterion specifies gradually decreasing collection efficiencies with increasing particle size, and has a d_{50} of 40 nm. The final filter collects the remaining airborne particles with a target collection efficiency of 100%.

2.1.1. Impactor stage

The target d_{50} for the impactor stage of the high-flow NRD sampler was 300 nm ± 5 nm. Three different nozzle sections, each having 12 round nozzles, were machined and tested to obtain the desired d_{50} (Table 1). Critical design dimensions, theoretical d_{50} and theoretical pressure drop of three nozzle sections were calculated for each nozzle section design. Also, design elements that affect d_{50} of an impactor, such as nozzle diameter (W_{nozzle}), dimensionless nozzle to plate distance S/W_{nozzle} (S is the nozzle to plate distance), dimensionless nozzle throat length T/W_{nozzle} (T is the nozzle throat length), the Reynolds number (Re) and jet velocity V were estimated following Marple and Willeke (1976). The nozzle Re was maintained between 500 and 3000 to obtain sharp cutoff characteristics. All three nozzle sections had a tapered inlet as illustrated in Fig. 1b and a T/W_{nozzle} ratio greater than 1 to obtain uniform airflow. The fabricated nozzle diameters were determined using an optical microscope (Leica Microsystems 02Q-522.101) and ImageJ software (1.6.0_24, NIH, Bethesda, MD, USA).

Prior to experimental testing, each nozzle section and the impaction plate were cleaned using an isopropanol pad (North Safety Products, 032525, RI, USA), and a small amount of grease was applied to the impaction plate to reduce particle bounce.

2.1.2. Diffusion stage

Polyurethane foam with a diameter of 37 mm and a porosity of 90 pores per inch (Crest Foam Industries Inc., NJ, USA) was used as the diffusion stage in the high-flow NRD sampler. The same foam was used previously in the low-flow NRD sampler (Mines et al., 2016). The diffusion stage consisted of two foam pieces (Fig. 1a), the upstream piece of foam was 5 cm long, whereas the downstream foam was varied in length to optimize collection efficiency. The length of the downstream piece was 0, 2, and 5 cm to achieve a total length of the diffusion stage of 5, 7, and 10 cm.

2.1.3. Final filter

A mixed cellulose ester (MCE) filter (37 mm, 5 µm pore size, SKC, 225–1938, CA, USA) supported with a cellulose support pad (SKC, 225-27, CA, USA) was used as a final stage (Fig. 1a). To reduce resistance to airflow, the support pad was modified by punching seven, evenly-spaced, 8-mm-diameter holes in a concentric ring 25 mm in diameter. This yielded an open area of 32.7% of the total pad area.

2.2. Collection efficiency

Collection efficiencies by size of the impactor stage, diffusion stage, and final filter were obtained individually using the experimental setup shown in Fig. 2. All collection efficiency tests were conducted with a flow rate of 10 L/min. A 0.9% salt solution (NaCl, 2F7123, Baxter Healthcare Co., Deerfield, IL, USA) aerosolized by a vibrating mesh nebulizer (Aeroneb Solo System, Aerogen, Ireland) was used to measure collection efficiencies in the size range from 20 nm to 700 nm. Dry and clean air regulated with a mass flow controller (MFC; MPC20, Porter Instrument, Hatfield, PA, USA) was delivered to a vibrating mesh nebulizer. Generated aerosol was passed through a silica diffusion dryer to ensure solid crystal salt particles and an ^{85}Kr charge neutralizer (3054, TSI, Shoreview, MN, USA) to render the charge distribution on the particles to a Boltzmann distribution. A 200-L coagulation chamber was used to increase particle size and to obtain a stable size distribution.

Particle number concentration by electrical mobility diameter was measured using scanning mobility particle sizer (SMPS; 3938, TSI, Shoreview, MN). The SMPS consisted of an electrostatic classifier (Model 3082), an advanced aerosol neutralizer (Model 3088), a long differential mobility analyzer (DMA, Model 3081A), and a condensation particle counter (CPC, Model 3788). The SMPS was set to a sampling flow rate of 0.3 L/min and a sheath flow rate of 3 L/min. Salt aerosol passed through an empty housing (bypass) and through a tested element (impactor, foam, or filter) at least three times each. For each design element and SMPS particle size bin, collection efficiency (η_c) was calculated as follows:

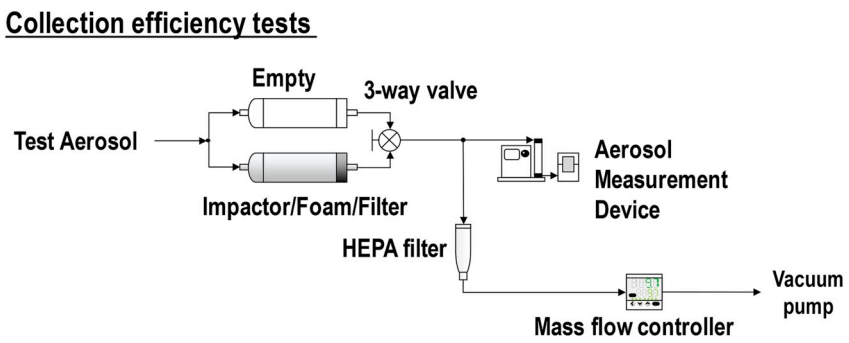

Fig. 2. Experimental setup used to measure collection efficiency of salt/glass microspheres for the impactor, foam, and final filter.

$$\eta_c = 1 - \frac{C_{element}}{C_{bypass}}, \tag{2.1}$$

where $C_{element}$ is an average number concentration exiting the impactor, foam, or filter; and C_{bypass} is an average number concentration exiting the empty housing. Collection efficiency of particles larger than 500 nm were measured using aerosolized glass microspheres (Spheriglass, 5000 A, Lot No: 080536476K, Potters Industries Inc., NJ, USA) by an Aerodynamic Particle Sizer (APS; 3321, TSI, Shoreview, MN). A fluidized bed generator (3400A, TSI Inc., Shoreview, MN, USA) was used to aerosolize the glass microspheres which were subsequently mixed with clean air (250 L/min) in a mixing chamber (0.64 m × 0.64 m × 0.66 m) and sampled in a separate sampling area (0.53 m × 0.64 m × 0.66 m). The particle size channels from the APS were converted from aerodynamic diameter to mobility diameter following Peters, Chein, Lundgren, and Keady (1993) using a shape factor of 1 and density of 2500 kg/m^3.

The collection efficiency of the diffusion stage was adjusted for the presence of the impactor operated with Nozzle Section 1. The adjustment was made because of excess pressure demands on the SMPS system when both impactor and foam were in series. The foam efficiency adjusted for the presence of the impactor was defined as $\eta_{f/i}$:

$$\eta_{f/i} = \eta_{foam} \times (1 - \eta_{impactor}). \tag{2.2}$$

The experimentally adjusted collection efficiency curves for the diffusion stage were compared to the NPM curve by applying the coefficient of determination, $R^2_{f/i}$, calculated as:

$$R^2_{f/i} = 1 - \frac{\Sigma(\eta_{f/i} - NPM)^2}{\Sigma(\eta_{f/i} - \eta_{f/i,avg})^2}, \tag{2.3}$$

where $\eta_{f/i,avg}$ is the average foam efficiency adjusted for the presence of the impactor .

2.3. Pressure drop

The experimental pressure drop across the impaction stage, diffusion stage, and final filter was measured using a pressure gauge (Wallace and Tiernan SN: 9481B, Lawrenceville, GA) at the flow rate of 10 L/min. Each design element's pressure drop was measured individually and then measured for a complete sampler.

2.4. Minimum sampling time

The minimum sampling time was based the metal mass that would be collected on the foam substrate after sampling at concentrations of 1/10th of the Occupational Exposure Limit (OEL) for a particular metal element. Metal content of the foam was measured using Inductively Coupled Plasma (ICP)-Mass Spectrometry (MS) (iCAP RQ ICP-MS, Thermo Fisher Scientific, MA, USA) analysis after microwave digestion of the foam using a Microwave Reaction System (MARS 6, CEM Corporation, Matthews, NC) following the NIOSH method 7302 (Ashley, 2016). The limits of quantification (LOQs) of cadmium (Cd), chromium (Cr), copper (Cu), iron (Fe), manganese (Mn), nickel (Ni), titanium (Ti), and zinc (Zn) were calculated as the mean blank concentration plus 10 times the standard deviation of the blanks (Shrivastava & Gupta, 2011). The LOQ represents the lowest amount of mass required to accurately distinguish sampled metals from background content of the media. An estimated minimum sampling time (t_{min}) needed when sampling at the flow rate Q = 10 L/min and at a concentration C equal to 1/10th of the Recommended Exposure Limit (REL) for titanium dioxide and 1/10th of the Threshold Limit Values (TLVs) for all other metals was calculated using the following equation:

$$t_{min} = \frac{LOQ}{C * Q}. \tag{2.4}$$

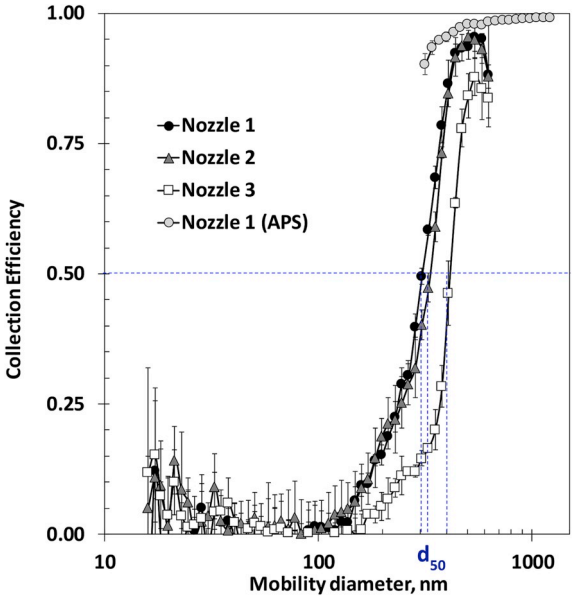

Fig. 3. Particle collection efficiency by particle mobility diameter for Nozzle Sections 1, 2, and 3. Nozzle Section 1 measured by SMPS and APS.

3. Results and discussion

3.1. Impactor stage

Collection efficiencies by particle mobility diameter for three impactor nozzle sections are shown in Fig. 3. The collection efficiency curves of all nozzle sections exhibited a similar behavior with a sharp increase from 0.01 (± 0.03) at 100 nm to 0.96 (± 0.03) for particles at 542 nm. Nozzle Section 1 met the target d_{50} at 305 nm whereas Nozzle Section 2 had d_{50} at 328 nm and Nozzle Section 3 had d_{50} at 406 nm (Fig. 3 and Table 1). Nozzle Section 1 was selected to be used in the final design of the high-flow NRD sampler due to its d_{50} being the closest to the target value of 300 nm. Collection efficiency for larger diameters (up to 2000 nm) was measured using the APS only for Nozzle Section 1 and was close to 100% (Fig. 3). These data show that particle bounce from the impaction plate is minimal. The collection efficiency of the APS was higher than that measured by the SMPS for particles from 310 nm to 400 nm. This discrepancy is thought to stem from differences in the density and shape factor of the salt and glass bead aerosol.

Larger jet diameters such as for Nozzle Section 3 (W_{nozzle} = 0.626 ± 0.008 mm) had higher precision, wheras smaller nozzle diameter as for Nozzle Section 1 (W_{nozzle} = 0.566 ± 0.144 mm) were difficult to make with high precision (Table 1). The fact that the sharpness of the collection efficiency curve was similar for Nozzle Section 1 and Nozzle Section 2 suggests that this change in precision had little influence on performance. Marple and Willeke (1976) recommended that the S/W_{nozzle} ratio should be greater than 1 for constant efficiency curves which was assured for all designed nozzle sections, ranging from 1.4 for Nozzle Section 2 to 1.73 for Nozzle Section 1. T/W_{nozzle} ratio greater than 1 was also obtained for all nozzle sections which should ensure uniform flow through the nozzles. Re number over 2000 was calculated for Nozzle Sections 1 and 2. The jet velocity, V was the highest for Nozzle Section 1 at 5447 cm/s and was greatly reduced to 2641 cm/s for the larger jet diameter of Nozzle Section 3.

The high-flow NRD impactor was designed with slightly different physical characteristics compared to the low-flow NRD sampler but both types of impactors met Marple and Willeke (1976) recommendations. For example, the S/W_{nozzle} ratio for the impactor of the 2.5 L/min NRD sampler was 1.9 whereas this ratio for Nozzle Section 1 used in high-flow NRD sampler was 1.73, and the Re number of the 2.5 L/min NRD impactor was 2212 whereas the Re of high-flow NRD impactor was 2057 (Cena et al., 2011). The high-flow NRD sampler design also included a tapered inlet whereas the 2.5 L/min NRD sampler did not (Cena et al., 2011). In comparison, PENS sampler's S/W_{nozzle} ratio of the impactor with their target d_{50} was 13.8 but the Re was below the recommend range (500–3000) at 385 (Tsai, Liu et al., 2012).

3.2. Diffusion stage

The impactor-adjusted collection efficiencies by size for the diffusion stages with foam depths of 5, 7, and 10 cm are shown in Fig. 4. The R^2 values calculated using Equation (2.3) for each of the foam depths were 0.92 for 10 cm, 0.96 for 7 cm, and 0.90 for 5 cm. The corresponding d_{50} for the foam depths of 10 cm, 7 cm, and 5 cm were 50 nm, 43 nm, and 32 nm, respectively. Collection efficiency of the diffusion stage adjusted by the impactor with Nozzle Section 1 was the closest match to the NPM criterion. As expected, the collection efficiency of the foam decreased with increasing particle size due to diffusion. For particles from 21 nm to 40 nm in size, the collection efficiency of the foam was 10% greater than the NPM criterion for foam depths of 7 cm and 10 cm. For particles around 100 nm in size the collection efficiency was approximately 0.20 and decreased to 0.05 for particles around 300 nm.

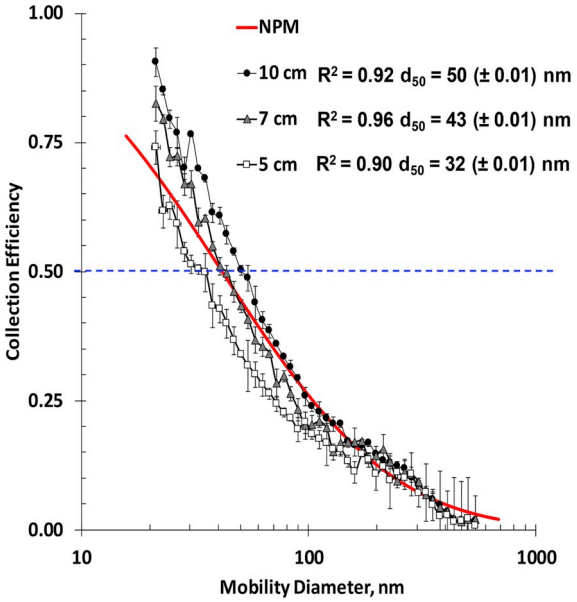

Fig. 4. Collection efficiencies by particle mobility diameter for different foam lengths. Efficiencies were adjusted for the presence of the impactor with Nozzle Section 1.

Due to the impactor adjustment, the collection efficiency was the lowest for particles larger than 300 nm. The foam depth of 7 cm in the diffusion stage had the highest R^2 value and provided d_{50} closest to the 40 nm target, hence it was selected to be used in the final design of the high-flow NRD sampler.

Achieving lower sampling times to meet metal LOQs for the NRD diffusion stage was the primary motivation for the development of the high-flow NRD sampler. The minimum sampling times required to reach LOQs for metals tested in this work at 1/10th exposure limit concentrations for the high-flow sampler were significantly reduced (almost in half for many metals and almost 4-fold for Ti) compared to the 2.5 L/min sampler (Table 2). These results were expected. The high-flow NRD sampler has four times higher flow rate in comparison to the 2.5 L/min sampler and can collect more sample in the same sampling time.

However, the LOQs for the high-flow NRD sampler were substantially larger than for the 2.5 L/min sampler due to the larger volume of foam required to achieve the NPM target collection efficiency (Table 2). This situation is unlike typical air sampling in which the same filter is used with different airflows. In filter sampling, the LOQ is constant because the filter does not change and sampling time is inversely related to flow rate alone. Future work should examine ways to reduce the LOQ of the media used in the diffusion stage as such a reduction would also shorten sampling times. The foam used in this work may be prewashed to remove impurities. Alternatively, different substrates could be used as diffusion stages.

3.3. Final filter

The collection efficiency by size was near the target of 100% for the final filter supported by the modified pad (Fig. 5). A slight dip

Table 2
Limits of quantification and minimum sampling times for the diffusion stage in low-flow (2.5 L/min) and high-flow (10 L/min) NRD samplers. Sampling times for 1/10th of the occupational exposure limit, OEL.

Element	LOQ, μg		OEL,[a] μg/m³	Minimum sampling time, min[b]	
	low flow	high flow		low flow	high flow
Cd	0.012	0.025	2	24.0	12.5
Cr	0.133	0.300	500	1.1	0.6
Cu	0.065	0.235	200	1.3	1.2
Fe	2.670	6.073	5000	2.1	1.2
Mn	0.088	0.270	20	17.6	13.5
Ni	0.031	0.083	1500	0.08	0.06
Ti	0.086	0.093	300	1.1	0.3
Zn	1.767	3.575	1607 [c]	3.5	2.2

[a] OELs of all elements except Ti are ACGIH TLVs (ACGIH, 2019); Ti OEL is the NIOSH REL (NIOSH, 2011).
[b] For airborne concentrations at 1/10th the OEL.
[c] TLV for zinc oxide, 2000 μg/m³, was adjusted for Zn only.

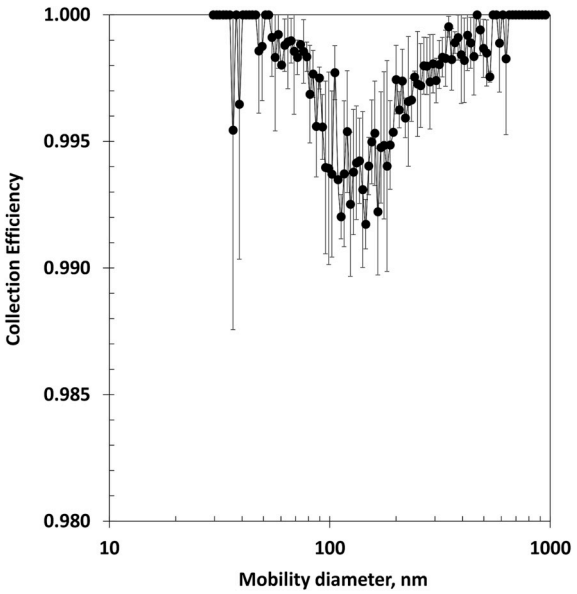

Fig. 5. Collection efficiency by mobility diameter of the final filter with a modified support pad.

in collection efficiency was observed for particles between 31 nm and 224 nm with the lowest collection efficiency at 0.992 ± 0.001 for 88 nm particles. The MCE filter had a substantial pressure drop of 3.0 kPa (12 in H_2O). The support pad pressure drop was 2.7 kPa (11 in H_2O) and it was decreased to 1.4 kPa (5.5 in H_2O) with the modification described in Methods section, while the pressure drop for a system of MCE filter and the pad decreased from 5.5 kPa (22 in H_2O) to 4.4 kPa (17.5 in H_2O) after this modification.

3.4. Design summary

The final design for high-flow NRD sampler consists of Nozzle Section 1 with d_{50} of 305 nm, 7-cm long polyurethane foam with d_{50} of 43 nm, and 5-μm pore size MCE filter with near 100% collection efficiency. The pressure drops for each component and the assembled sampler are shown in Table 3. The impactor stage had a pressure drop of 4.2 kPa (16.9 in H_2O). The diffusion stage had the lowest pressure drop of all NRD stages at 1.7 kPa (6.8 in H_2O). The pressure drop across the final filter with the support pad was 4.4 kPa (17.5 in H_2O). With all components, the complete sampler had a pressure drop of 8.5 kPa (34 in H_2O), which is substantially less than the sum of the pressure drop for individual components. This difference is attributed to the pressure drop of the housing, which was approximately 1 kPa. The pressure drop of the complete sampler cannot be handled by commercial personal pumps (e.g., Gilian 12 from Sensidyne, St Petersburg, FL, USA). Thus, the high-flow NRD sampler can only be used with such personal pumps when operated without the final filter. Other options to decrease NRD sampler pressure drop are to use a larger filter (e.g. 47 mm in diameter) or to use a filter with larger pore size (e.g. 8 μm), which may reduce the pressure drop but may also lower collection efficiency.

A limitation of this work was that we did not test the impactor under non-ideal conditions. Specifically we did not evaluate clogging of the impactor nozzles with highly fractal or large diameter particles. We also did not determine the effect of particle loading on the impactor cutoff curve. We did not characterize the particle loss in the dome-shaped inlet, which could be the subject of future work. Clogging and particle loading may be an issue under field conditions due to the small diameter nozzles and the absence of a size-selective inlet. Such an inlet would remove larger particles from the airstream, thereby protecting the nozzles from clogging and the plates from over-loading.

4. Conclusions

A high-flow NRD sampler was designed and tested with a flow rate of 10 L/min. The collection efficiency of the high-flow NRD

Table 3
Summary of all elements for the final design of high-flow NRD sampler.

	d_{50}, nm	R^2	Δ P, kPa (in H_2O)
Impactor stage (Nozzle 1)	305	NA	4.2 (16.9)
Diffusion stage (7 cm)	43	0.96	1.7 (6.8)
Final filter with support pad (5 μm MCE)	NA	NA	4.4 (17.5)
Complete Sampler	NA	NA	8.5 (34)

sampler matched well to the NPM criterion curve that mimics the respiratory deposition curve for the nanoparticles. The sampler can be used in low aerosol concentration environments and requires less time to collect enough mass to quantify aerosol composition by ICP-MS when compared to 2.5 L/min NRD sampler. The high-flow NRD sampler facilitates lower detection limits and helps filling a critical gap of obtaining personal nanoparticle exposure assessments in the workplaces.

Acknowledgements

This research was funded by generous support from the National Institute for Occupational Safety and Health Grant No. R01OH010238 and the Heartland Center for Occupational Safety and Health Training Grant No. T42OH008491.

Appendix A. Supplementary data

Supplementary data to this article can be found online at https://doi.org/10.1016/j.jaerosci.2019.04.019.

References

ACGIH (2019). *Threshold limit values and biological exposure indicies.* Cincinnati, OH: American Conference of Governmental Industrial Hygienists.
Ashley, K. (2016). *Elements by ICP (microwave digestion), method 7302. NIOSH manual of analytical methods (NMAM)*.
Cena, L. G., Anthony, T. R., & Peters, T. M. (2011). A personal nanoparticle respiratory deposition (NRD) sampler. *Environmental Science & Technology, 45*(15), 6483–6490.
Marple, V. A., & Willeke, K. (1976). Impactor design. *Atmospheric Environment, 10*(10), 891–896.
Mines, L. W., Park, J. H., Mudunkotuwa, I. A., Anthony, T. R., Grassian, V. H., & Peters, T. M. (2016a). Porous polyurethane foam for use as a particle collection substrate in a nanoparticle respiratory deposition sampler. *Journal Aerosol Science Technology, 50*(5), 497–506.
Mines, L. W. D., Park, J. H., Mudunkotuwa, I. A., Anthony, T. R., Grassian, V. H., & Peters, T. M. (2016b). Porous polyurethane foam for use as a particle collection substrate in a nanoparticle respiratory deposition sampler. *Aerosol Science and Technology, 50*(5), 497–506.
NIOSH (2011). *Current intelligence bulletin 63: Occupational exposure to titanium dioxide.* DHHS (NIOSH) Publication Number 2011-2160.
NIOSH (2013). *Current intelligence bulletin 65: Occupational exposure to carbon nanotubes and nanofibers.* DHHS (NIOSH) Publication Number 2013-2145.
Peters, T., Chein, H., Lundgren, D., & Keady, P. (1993). Comparison and combination of aerosol size distributions measured with a low pressure impactor, differential mobility particle sizer, electrical aerosol analyzer, and aerodynamic particle sizer. *Aerosol Science and Technology, 19*(3), 396–405.
Shrivastava, A., & Gupta, V. (2011). Methods for the determination of limit of detection and limit of quantitation of the analytical methods. *Chronicles of Young Scientists, 2*(1), 21–25.
Thompson, D., Chen, S.-C., Wang, J., & Pui, D. Y. (2015). Aerosol emission monitoring and assessment of potential exposure to multi-walled carbon nanotubes in the manufacture of polymer nanocomposites. *Annals of Occupational Hygiene, 59*(9), 1135–1151.
Thongyen, T., Hata, M., Toriba, A., Ikeda, T., Koyama, H., Otani, Y., et al. (2015). Development of a PM0. 1 personal sampler for evaluation of personal exposure to aerosol nanoparticles. *Journal Aerosol Air Quality Research, 15*(1), 180–187.
Tsai, C.-J., Liu, C.-N., Hung, S.-M., Chen, S.-C., Uang, S.-N., Cheng, Y.-S., et al. (2012). Novel active personal nanoparticle sampler for the exposure assessment of nanoparticles in workplaces. *Environmental Science & Technology, 46*(8), 4546–4552.
Zhou, Y., Irshad, H., Tsai, C.-J., Hung, S.-M., Cheng, Y.-S., & Impacts (2014). Evaluation of a novel personal nanoparticle sampler. *Journal of Environmental Sciences: Processes, 16*(2), 203–210.